Proceedings of the 2nd WRC Symposium
on Advanced Robotics and Automation 2019
Beijing, China, August 21, 2019

Research on Wheel-wall Gap Calculation Method for Four-Magnetic Wheel Wall-Climbing Robot Walking on Cylindrical Tank

Taoyu Han, Ruiming Qian

***Abstract*—In order to better study the adsorption property of the magnetic wheeled wall-climbing robot for its stably walking on the wall of the cylindrical tank, the calculation method of the gap from the magnetic wheel to tank wall is proposed. The three-wheel or four-wheel contact mode of the robot on the cylindrical tank wall is analyzed, and the contact points between magnetic wheels and the tank wall is determined. The position and orientation of the robot on the tank wall are described by coordinate transformation, and the change law of wheel-wall gap along the wheel axis is established by geometric method. The whole solution process is numerically calculated by MATLAB finally. The results can be used in the design of magnetic wheel structure and magnetic force.**

***Key words*—four-magnetic wheeled wall-climbing robot, Cylindrical tank, Coordinate transformation, Wheel-wall gap.**

I. INTRODUCTION

At present, more and more steel tanks are used in petroleum, chemical and other industries to store flammable, explosive or toxic substances. Once leakage occurs, it will cause great harm and loss [1]. Therefore, regular inspection of the tank body is necessary. The current detection method is basically manual operation, but the method has the disadvantages of high cost, high labor intensity and high risk. With the rapid development of robotics, more and more research departments have begun to develop wall-climbing robots, hoping to replace manual for tank detection. The permanent magnetic wheeled wall-climbing robot has the characteristics of reliable adsorption, simple structure and flexible movement, and has wide application prospects in the detection of steel tank wall surface [2][3][4][5][6][7].

The adsorption function is the primary function of the wall-climbing robot, and it is also the key factor affecting the working performance of the wall-climbing robot [8]. Therefore, in some literatures, the stability analysis and simulation of the magnetic adsorption of the permanent magnetic wheeled wall-climbing robot are carried out. Zhang designed a wheeled wall-climbing robot, studied the adsorption stability, and used ANSOFT MAXWELL to analyze and optimize the adsorption device [9]. In refer [10], a wheeled wall-climbing robot was designed for the detection of cylindrical tanks, the stability analysis and numerical simulation of the robot was carried out, and obtained the minimum adsorption force required by the robot to work stably. Cai designed a magnetic wheeled wall-climbing robot, analyzed the possible sliding and overturning that may occur in the robot, obtained the minimum adsorption force required by the robot, and simulated a magnetic wheel by ANSOFT MAXWELL [11]. In refer [12], a permanent magnetic wheeled wall-climbing robot is proposed for the derusting work of steel wall. The calculation and analysis of magnetic adsorption force are carried out, and the safety of the obtained adsorption force was verified by sliding and overturning. In the literatures mentioned above, when analyzing and simulating the magnetic adsorption force, the wall are all planes. In this case, the magnetic wheels and the wall are in line contact. However, when the magnetic wheeled wall-climbing is used for tank detection, the wall is curved surface, the magnetic wheels and the wall are in point contact, At this time, there is a gap between the wheel and the tank wall except the contact point, which increases the gap between the permanent magnet and the wall, and has a great influence on the adsorption force [13].

The research object of this paper is a wall-climbing robot with four magnetic wheels. The four magnetic wheels are parallel to each other and fixed on both sides of the robot body. In order to more accurately solve the adsorption force required by the wall-climbing robot to move stably on the tank wall, it is necessary to solve the gap from magnetic wheel to the tank wall. In this paper, for the cylindrical tank, the contact points between magnetic wheels and the tank wall are represented by coordinates by means of coordinate transformation. The relationship is established by analytic geometry method to solve the gap between magnetic wheel and tank wall. Finally, a practical example is calculated by MATLAB, and the gaps between magnetic wheel and the tank wall under different attitudes of the wall climbing robot are obtained, which can be used in the design of magnetic wheel structure and the analysis of magnetic force.

II. COORDINATE SOLUTION OF THE CONTACT POINTS BETWEEN THE ROBOT AND THE CYLINDRICAL TANK WALL

A. Establishment of Coordinate System

In order to make the analysis simple, the following assumptions are made: the wheel is simplified as a disc; wheels and the wall are rigid bodies without deformation, and the contact between the wheel and the tank wall is point contact between two cylindrical surfaces.

The distance between the front and rear magnetic wheels is l, the distance between the left and right magnetic wheels is b, and the width of the wheel is a. The magnetic wheels are labeled in a counterclockwise direction, the inner points of the bottom of four magnetic wheels form a rectangle, and the

Taoyu Han is with the College of Mechanical Engineering, Southeast University, Nanjing, Jiangsu, China. (e-mail: hty199501@163.com).
Ruiming Qian is with the College of Mechanical Engineering, Southeast University, Nanjing, Jiangsu, China. (e-mail: rmqian@seu.edu.cn).

978-1-7281-5552-4/19/$31.00 ©2019 IEEE

Authorized licensed use limited to: Massey University. Downloaded on August 08,2020 at 06:35:05 UTC from IEEE Xplore. Restrictions apply.

coordinate system C_m is fixed on the rectangle. The origin o_m is the center of the rectangle, the coordinate axis x_m is perpendicular to the rectangle outward, and the coordinate axis z_m is parallel to the front and rear wheels, the direction points to wheels 1 and 2, as shown in Fig. 1. The coordinates of the inner points of the bottom of the four magnetic wheels can be expressed as $A_{im}(x_{im}, y_{im}, z_{im})$, i=1, 2, 3, 4.

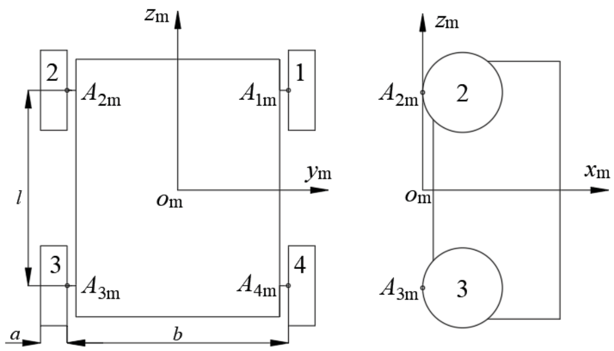

(a) (b)

Figure 1. Setting of robot coordinate system.

The coordinate system C_f is fixed at the bottom of the cylindrical tank, the origin o_f is the center of the bottom circle, and z_f is upward along the axis of the tank, as shown in Fig. 2. When the cylindrical radius is *r* and the height is *h*, the equation for the cylindrical surface is:

$$x_f^2 + y_f^2 = r^2 \tag{1}$$

$$0 \le z_f \le h \tag{2}$$

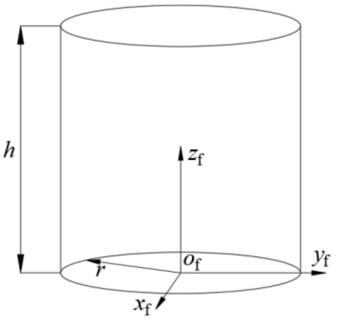

Figure 2. Setting of tank coordinate system.

B. Analysis of Contact Between Magnetic Wheels and The Cylindrical Tank Wall

When the robot is adsorbed on the cylindrical tank wall, if the coordinate axis z_m is parallel or perpendicular to z_f , the four magnetic wheels are all in contact with the tank wall; otherwise, only three magnetic wheels are in contact with the tank wall and one wheel is lifted. In the latter case, as shown in Fig. 3, in the view facing the direction of the robot body, the distance from the wheel to the axis of the tank body in the horizontal direction is represented by d. Due to the cylindrical structure of the tank, and under the action of magnetic adsorption force, the smaller the d, the more the wheel is adsorbed on the tank. Thus, the two wheels close to the axis of the tank must be in contact with the tank wall, and only one wheel of the two wheels relatively far away from the axis of the tank contacts on the tank wall.

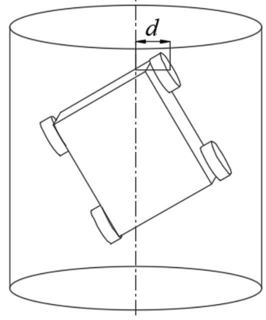

Figure 3. Three wheels contact on the wall

Suppose that the alternate angle between the coordinate axis z_f forward along the counterclockwise direction to the coordinate axis z_m forward is expressed by θ, as shown in Figure 3. When θ=0, π/2, π, 3π/2, the four magnetic wheels are in contact with the cylindrical tank wall.

When $\theta \in$ (0, π/2)(Fig. 4a) or $\theta \in$ (π, 3π/2) (Fig. 4b), wheels 1, 3 are closer to the tank axis, thus contacting on the tank wall, and one of wheels 2 and 4 is lifted.

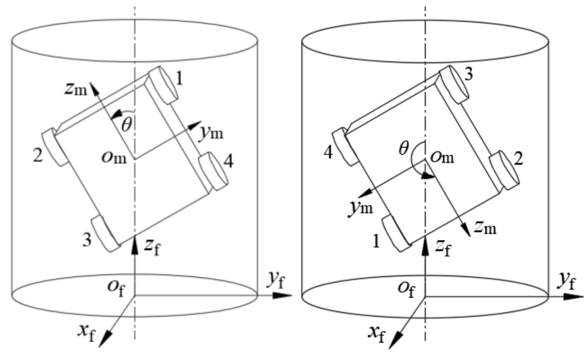

(a) $\theta \in (0, \pi/2)$ (b) $\theta \in (\pi, 3\pi/2)$

Figure 4. Wheels 1, 3 contact on the wall, one of wheels 2, 4 is lifted.

When $\theta \in$ (π/2, π) (Fig. 5a) or $\theta \in$ (3π/2, 2π) (Fig. 5b), the wheels 2, 4 are closer to the tank axis, thus contacting on the tank wall, and one of the wheels 1 and 3 is lifted.

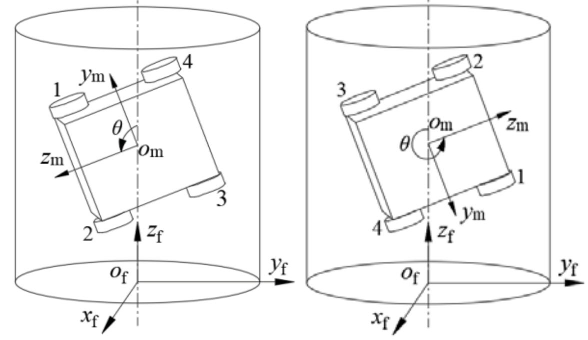

(a) $\theta \in (\pi/2, \pi)$ (b) $\theta \in (3\pi/2, 2\pi)$

Figure 5. Wheels 2, 4 contact on the wall, one of wheels 1, 3 is lifted.

Authorized licensed use limited to: Massey University. Downloaded on August 08,2020 at 06:35:05 UTC from IEEE Xplore. Restrictions apply.

C. Analysis of the Contact Points Between Magnetic Wheels and The Cylindrical Tank Wall

The following is mainly to analyze the contact points of the magnetic wheels and the cylindrical tank wall at the time of $\theta \in (0, \pi/2)$, and then give the solution process of the pose transformation matrix. When the robot is placed, the wheels 1, 2, and 3 are contacted, and the wheel 4 is lifted. The coordinates of the contact points between wheels 1, 2, 3 and the tank wall are expressed as $A_{if}(x_{if}, y_{if}, z_{if})$, i=1, 2, 3.

According to the structural size of the robot, it can be concluded that the coordinates of the inner points of the bottom of the four magnetic wheels is: $A_{1m}(0, b/2, l/2)$, $A_{2m}(0, -b/2, l/2)$, $A_{3m}(0, -b/2, -l/2)$, $A_{4m}(0, b/2, -l/2)$.

Next, we need to determine the coordinates of each contact point in C_f. First, the inner point of the bottom of wheel 1 is chosen as the first contact point A_{1f}, any position of this point on the tank wall will not affect the attitude of the robot, just satisfy the conditions:

$$x_{1f}^2 + y_{1f}^2 = r^2 \tag{3}$$

$$b^2 + l^2 \le z_{1f} \le h - b^2 - l^2 \tag{4}$$

The coordinate of the contact point A_{2f} of wheel 2 is determined by the coordinate of A_{1f}. At this time, the inner point of the bottom of wheel 2 is in contact with the tank wall, and the coordinate of A_{2f} needs to satisfy the conditions:

$$(x_{2f} - x_{1f})^2 + (y_{2f} - y_{1f})^2 + (z_{2f} - z_{1f})^2 = b^2 \tag{5}$$

$$x_{2f}^2 + y_{2f}^2 = r^2 \tag{6}$$

According to (5) and (6), we can get:

$$(x_{2f} - x_{1f})^2 + (\sqrt{r^2 - x_{2f}^2} - y_{1f})^2 + (z_{2f} - z_{1f})^2 = b^2 \tag{7}$$

When z_{2f} is selected, x_{2f} is obtained and the coordinate of A_{2f} on the tank wall is obtained. Obviously, the choice of z_{2f} will affect the attitude angle θ of the robot.

The coordinate of the contact point between wheel 3 and the tank wall need to be determined at last. During the change of θ from 0 to $\pi/2$, the contact point of wheel 3 on the tank wall will change. Initially, the contact point is the inner point of the bottom, with the change of θ, the contact point begins to shift from the inside to the outside, eventually the contact point becomes the outer point of wheel 3. Due to the limited space, this paper only analyzes the inner point of the bottom of wheel 3 contacts on the tank wall, and the coordinate of the contact point can be determined by the following equations:

$$x_{3f}^2 + y_{3f}^2 = r^2 \tag{8}$$

$$(x_{3f} - x_{1f})^2 + (y_{3f} - y_{1f})^2 + (z_{3f} - z_{1f})^2 = b^2 + l^2 \tag{9}$$

$$(x_{3f} - x_{2f})^2 + (y_{3f} - y_{2f})^2 + (z_{3f} - z_{2f})^2 = l^2 \tag{10}$$

According to the above, the contact point of wheel 3 on the tank wall will change with the change of θ, and the change of θ depends on the change of z_{2f}. In order to solve the gap between the magnetic wheel and the tank wall when wheels 1, 2 and 3 are all in contact with the tank wall with the inner point of the bottom, the range of z_{2f} when wheel 3 is in contact with the inner point of the bottom is needed to be determined.

When wheels 1, 2, and 3 are all in contact with the tank wall with the inner point of the bottom, assuming that the line passing through points A_{1f} and A_{2f} is l_1, and the line passing through A_{3f} is l_3 parallel to l_1, then the line l_3 must intersect the tank at two points. In addition to the contact point A_{3f}, the other intersection point is $A'_{3f}(x'_{3f}, y'_{3f}, z'_{3f})$, and the two intersection points satisfy the condition $z'_{3f} > z_{3f}$, so that it can be used as a basis for judging. When z_{2f} changes from the initial value to a certain value, the condition is no longer satisfied, then the contact point between wheel 3 and the tank wall is no longer the inner point of the bottom of wheel 3, and the interval of the change of z_{2f} is the value range of z_{2f}.

According to the coordinates of A_{1f}, A_{2f} and A_{3f}, the direction vector along the positive direction of z_m can be obtained, and the direction vector along the positive direction of z_f can be easily obtained, the angle θ between the two direction vectors can be solved by the cosine theorem. Then we can get the range of θ according to the range of z_{2f}.

III. The Transformation Matrix of the Pose of the Robot Relative to the Cylindrical Tank Wall

It is known that the position vector of the contact points in C_m is $\boldsymbol{a}_i^m = [x_{im}, y_{im}, z_{im}]^T$, and the position vector of the contact points in C_f is $\boldsymbol{a}_i^f = [x_{if}, y_{if}, z_{if}]^T$, i=1, 2, 3.

The pose of C_m relative to C_f can be expressed as a matrix of 4x4:

$$T = \begin{bmatrix} \boldsymbol{r}_0 & R \\ 0 & 1 \end{bmatrix} \tag{11}$$

Where $\boldsymbol{r}_0 = [x_0, y_0, z_0]^T$ is the position vector of the origin o_m of C_m in C_f, the contact points of wheel 1 and wheel 3 are the inner points of the bottom, then we can get $\boldsymbol{r}_0 = [\frac{x_{1f} + x_{3f}}{2}, \frac{y_{1f} + y_{3f}}{2}, \frac{z_{1f} + z_{3f}}{2}]^T$, R is the rotation matrix of the attitude of C_m relative to C_f.

The known vector relationship is:

$$\boldsymbol{a}_i^f = \boldsymbol{r}_0 + R\boldsymbol{a}_i^m \tag{12}$$

Substituting the determined data into (12), and according to the property of the rotation matrix, R can be obtained:

Authorized licensed use limited to: Massey University. Downloaded on August 08,2020 at 06:35:05 UTC from IEEE Xplore. Restrictions apply.

$$R = \begin{bmatrix} \dfrac{\sqrt{b^2l^2 - l^2(x_{1f}-x_{2f})^2 - b^2(x_{2f}-x_{3f})^2}}{bl} & \dfrac{x_{1f}-x_{2f}}{b} & \dfrac{x_{2f}-x_{3f}}{l} \\ \dfrac{\sqrt{b^2l^2 - l^2(y_{1f}-y_{2f})^2 - b^2(y_{2f}-y_{3f})^2}}{bl} & \dfrac{y_{1f}-y_{2f}}{b} & \dfrac{y_{2f}-y_{3f}}{l} \\ \dfrac{\sqrt{b^2l^2 - l^2(z_{1f}-z_{2f})^2 - b^2(z_{2f}-z_{3f})^2}}{bl} & \dfrac{z_{1f}-z_{2f}}{b} & \dfrac{z_{2f}-z_{3f}}{l} \end{bmatrix} \tag{13}$$

And the transformation matrix T can be obtained by substituting $\boldsymbol{r}_0$ and R into (12).

IV. SOLUTION OF THE GAP BETWEEN MAGNETIC WHEEL AND TANK WALL

According to the obtained transformation matrix T, the coordinate of a point of the bottom of the magnetic wheel in C_{m} can be converted into the coordinate $D(x_{df}, y_{df}, z_{df})$ in C_f, and then the gap from this point to the tank wall can be solved.

According to the above, the coordinates of the contact points A_{1f}, A_{2f}, A_{3f} between wheels 1, 2, 3 and the tank wall can be solved. From these three points, a plane can be determined, and the normal vector of the plane is expressed as: $\boldsymbol{n} = (A, B, C)$. Making a line as the normal of the plane which passing through the point D. The intersection of the normal and the tank wall is E, then the gap between D and E is the gap we need. The normal equation is:

$$\frac{x_f - x_{df}}{A} = \frac{y_f - y_{df}}{B} = \frac{z_f - z_{df}}{C} \tag{14}$$

According to (3), (4) and (14), the intersection coordinate $E(x_{ef}, y_{ef}, z_{ef})$ of normal and tank wall can be obtained, then we can get the gap from the magnet wheel to the tank wall is:

$$\delta = \sqrt{(x_{df}-x_{ef})^2 + (y_{df}-y_{ef})^2 + (z_{df}-z_{ef})^2} \tag{15}$$

V. NUMERICAL SIMULATION

The size parameters of the magnetic wheeled wall-climbing robot are as follows: l=220mm, b=230mm, a=30mm. The radius r of the cylindrical tank is 3000mm and the height h is 6000mm. According to size parameters, it can be concluded that the coordinates of the inner points of the bottoms of the four magnetic wheels is: A_{1m} (0, 115, 110), A_{2m} (0, -115, 110), A_{3m} (0, -115, -110), A_{4m} (0, 115, -110).

Next, the coordinates of each contact point in C_f are determined according to the conditions given in the foregoing, and in the case of $\theta \in (0, \pi/2)$, wheels 1, 2, 3 are in contact with the tank wall. First, the coordinate of the point A_{1f} are selected according to (3) and (4), the coordinate of A_{1f} is taken as (3000, 0, 2000). When the value of z_{2f} is selected, x_{2f} is obtained from (7), and the coordinate of A_{2f} can be obtained. It is known that θ depends on the selection of z_{2f}, when $\theta \in (0, \pi/2)$, $z_{2f} \in (2000, 1700)$. According to the judging condition that the inner point of the bottom of wheel 3 is the contact point, it can be calculated by MATLAB that when wheels 1, 2, and 3 are all contact with the tank wall with the inner side of the bottom, $z_{2f} \in (2000, 1894]$, and the alternate angle $\theta \in (0, 27.4°]$. Finally, the coordinate of the contact point can be obtained by (8), (9), (10).

When the robot is in a certain attitude, from the inside to the outside along the width direction of the bottom of the magnetic wheel, the gap from the magnetic wheel to the tank wall should be gradually increased. Then we use the MATLAB to do the simulation calculation. Fig. 5 show the gaps of each magnetic wheel along the width direction to the tank wall when θ=5°. The coordinates of contact points are: A_{1f} (3000, 0, 2000), A_{2f} (2991.25, -228.96, 1979.97), A_{3f} (2992.65, -209.84, 1760.81).

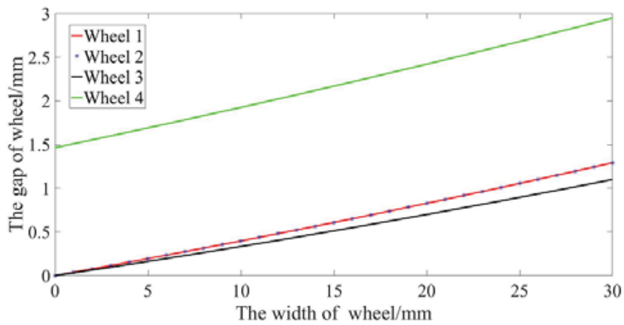

Figure 6. The gap of the wheel along the width to the tank wall.

It can be seen from the Fig. 6, from the inside to the outside along the width direction of the bottom of the magnetic wheel, the gap from the magnetic wheel to the tank wall is getting larger and larger, tends to linear variation, and the gap from the outermost point of the magnetic wheel to the tank wall is the largest. The gap from the outermost points of wheels 1 and 2 to the tank wall is almost the same, being 1.291 mm, and the gap from the outermost side of wheel 3 to the tank wall is slightly smaller than wheels 1, 2, which is 1.1 mm. Because wheel 4 is in the lifting state, the gap from the outermost side to the tank wall is the largest, being 2.948 mm, which is two to three times the gap from the outermost point of the other wheels to the tank wall.

According to the calculation, when wheels 1, 2, 3 are in contact with the tank wall with the inner point of the bottom, $\theta \in [0, 27.4°]$. Fig. 6 show the variation of the maximum gaps between each magnetic wheel and the tank wall.

Authorized licensed use limited to: Massey University. Downloaded on August 08,2020 at 06:35:05 UTC from IEEE Xplore. Restrictions apply.

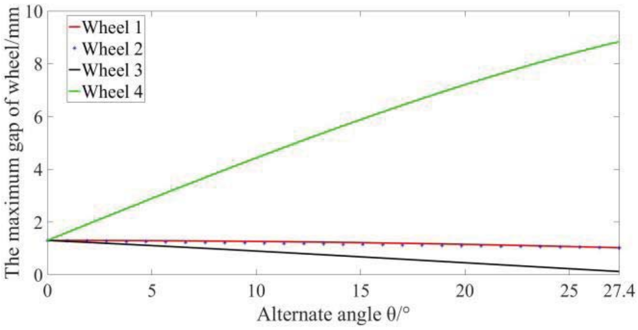

Figure 7. Maximum gap from wheel to the tank wall in different attitudes.

By changing the value of z_{2f} in the coordinate of A_{2f} to change θ, the change curve of the maximum gaps from the bottom of the magnetic wheels to the tank wall are obtained. It can be seen from the Fig. 7, when θ=0°, the gap between the four magnetic wheels and the tank wall is the same, which is 1.031 mm. The gaps from the three contact wheels 1, 2, and 3 to the tank wall decrease gradually with the increase of θ, and the gap between wheel 3 and the tank wall decreases faster than wheels 1 and 2, but the gap between the non-contact wheel 4 and the tank wall increases gradually. The wheels 1, 2, and 3 all have the largest gap to the tank wall at θ=0°, and the gap from wheel 4 to the tank wall at θ=27.4° is the largest, which is 8.838 mm, much larger than the gaps from wheels 1, 2 and 3 to the tank wall. It can be seen that the change of the attitude of the robot has a greater influence on the non-contact wheel.

VI. Conclusion

This paper analyses the situation of wall-climbing robot adsorbing on cylindrical tank. The contact mode and contact points of the robot on cylindrical tank are determined, the position and orientation of the robot on the tank wall are described by coordinate transformation, and the calculation method of the gap between magnetic wheel and the tank wall is given. Finally, we use MATLAB to simulate the example, and the following results are obtained:

(1) When the robot is in a certain pose, the gaps from inside to outside along the width direction of the four magnetic wheels to the tank wall increased gradually, and tends to linear variation. The changes of wheels 1 and 2 are almost the same.

(2) When the three contact wheels are in contact with the tank wall with the inner point of the bottom, the alternate angle θ changes from the initial value. The gaps from the three contact wheels to the tank wall decrease gradually with the increase of θ, and the gap from the non-contact wheel to the tank wall increases gradually. The gap between the non-contact wheel and the tank wall is much larger than the contact wheel.

The main purpose of this paper is to provide a basis for the design of magnetic wheel structure and the analysis of magnetic force. Because the gap between the magnetic wheel and the tank wall has a great influence on the magnetic force, the solution of the gap is very meaningful and need to continue research.

References

[1] Wang Congliang. Reasons and Measure for the Explosion of Oil Tank[J]. Guangdong Chemical Industry, 2010, 37(10): 211-212. (in Chinese)

[2] Fei Y, Zhao X, Wan J. Motion analysis of a modular inspection robot with magnetic wheels[C]//2006 6th World Congress on Intelligent Control and Automation. IEEE, 2006, 2: 8187-8190.

[3] Zhang D, Chen J, Li Z. An omni-directional wall-climbing microrobot with permanent-magnetic wheels actuated by electromagnetic micromotors[J]. Robot, 2011 (6): 12.

[4] Okamoto J, Grassi V, Amaral P F S, et al. Development of an Autonomous Robot for Gas Storage Spheres Inspection[J]. Journal of Intelligent & Robotic Systems, 2012, 66(1-2): 23-35.

[5] Espinoza R V, de Oliveira A S, de Arruda L V R, et al. Navigation's stabilization system of a magnetic adherence-based climbing robot[J]. Journal of Intelligent & Robotic Systems, 2015, 78(1): 65-81.

[6] Fischer W, Tâche F, Siegwart R. Magnetic wall climbing robot for thin surfaces with specific obstacles[C]//Field and Service Robotics. Springer, Berlin, Heidelberg, 2008: 551-561.

[7] Cho C S, Kim J D, Lee S G, et al. A study on automated mobile painting robot with permanent magnet wheels for outer plate of ship[C]//IEEE ISR 2013. IEEE, 2013: 1-4.

[8] Yuan Shuo, Liu Tianyu. Finite Element Analysis of Permanent Magnet Adsorption Unit for Electric Robot Based on Ansoft [J]. Electric Machines & Control Application, 2018 (2): 14. (in Chinese)

[9] Zhang Xiaosong. Research on Wall-Climbing Robot of Wheel-Shaped Suspended Magnetic Adsorption [D]. Harbin Institute of Technology, 2012, 2. (in Chinese)

[10] Liu Jigang, Tang Donglin, Jia Pinyuan. Stability Analysis of Wheeled Ultrasonic Testing Climbing Robot [J]. Machine Design and Research, 2016, 32(5): 25-30. (in Chinese)

[11] Cai J, He K, Fang H, et al. The design of permanent-magnetic wheeled wall-climbing robot[C]//2017 IEEE International Conference on Information and Automation (ICIA). IEEE, 2017: 604-608.

[12] Kong Hui. Study of the body structure of steel-wall-climbing robot[D]. Shandong University of Science and Technology, 2012. (in Chinese)

[13] Bisht R S, Pathak P M, Panigrahi S K. Experimental investigations on permanent magnet based wheel mechanism for safe navigation of climbing robot[J]. Procedia computer science, 2018, 133: 377-384.

Authorized licensed use limited to: Massey University. Downloaded on August 08,2020 at 06:35:05 UTC from IEEE Xplore. Restrictions apply.